

## DYNAMICALLY LOADED CYLINDRICAL JOURNAL BEARING WITH RECESS

Stanislaw Strzelecki<sup>1)</sup>, Sobhy M.Ghoneam<sup>2)</sup>

<sup>1)</sup> Department of Machine Design K-18

Technical University of Lodz

90-924 Lodz, Stefanowskiego Str. 1/15, Poland

Phone: (4842) 312239, fax: (4842) 6367489; e-mail: strzelec@pkml.p.lodz.pl

<sup>2)</sup> Mechanical Design & Production Engineering Department,

Faculty of Engineering

Menoufya University, Shebin-el-kom, EGYPT

e-mail: s.ghoneam@egyptcultural.pl

### Abstract

*Journal bearings which are dynamically loaded operate not only in internal combustion engines but also in, e.g. needle punching machines applied in textile machinery. Both applications are characterized by heavy dynamic load. Performances of bearing can be changed by variations of bearing bores. One of these variations is the recess of the depth of micrometers which is placed at assumed position on the bearing peripheral. An effect of this recess on the bearing performances is investigated by calculation of journal centre trajectory.*

*The numerical, coupled solution of geometry, Reynolds, energy and viscosity equations has allowed the determination of oil film resultant force and the journal centre trajectory of bearing with the recess. For saving the time of computation the isothermal oil film in the finite length bearing was assumed.*

### 1. Introduction

There are different branches of industry which apply dynamically loaded journal bearings. Heavy loaded by dynamic forces are the journal bearings of internal combustion engines [1-3] or the bearings of needle punching machines [1,4]. Both, engines and needle punching machines are more and more sophisticated with high parameters of operation as revolutions and loads. They are equipped in the systems of continuous monitoring of engines operating parameters or technological parameters of stitching and sensitive nodes of mechanisms of needle punching machine.

Needle punching machines have the driving system of stitching bench driven by crank-crosshead mechanism with the eccentric drive operating in dynamically loaded cylindrical journal bearings [1,4]. The demands for an increased efficiency require the application of new types of high speed, dynamically loaded bearings.

The recess of the depth of micrometers which is placed on the bearing peripheral can affect the journal centre trajectory. The wear of bearing generates the recess in determined part of bearing too.

The paper introduces the journal centre trajectories of bearings with and without the recess. Isothermal solution of Reynolds equation for obtaining the oil film resultant force and journal centre trajectory was applied. In calculation the different depth and orientation of recess on the bearing peripheral were assumed too.

## 2. The bearing loads

Two types of load, one characteristic for the internal combustion engine bearings [5] and another one of needle punching machine [4] have been considered. On the main bearings of needle punching machine acts the resultant inertia force of masses being in rotational movement and masses in the plane-back motion. The value of this resultant according to [1.4] is determined by following relation:

$$W = m_p r \cdot \omega^2 \sqrt{\beta^2 + (1 - 2\beta) \cos^2 \varphi + 2(1 - \beta) \lambda \cos \varphi \cos 2\varphi + \lambda^2 \cos^2 2\varphi} \quad (1)$$

where:  $m_p$  - mass in plane-back motion,  $r$  - crank radius,  $\omega$  - angular velocity of shaft,  $\beta$  - balance coefficient of masses in the plane-back motion,  $\varphi$  - angle of shaft rotation,  $\lambda = r/l$ ,  $l$  - length of connecting rod.

Formula (1) gives the total inertia force of the first and second order. The direction of non-balanced inertia force is determined from the relation (2):

$$\operatorname{tg} \theta = (-\beta \cdot \sin \varphi) / [(1 - \beta) \cdot \cos \varphi + \lambda \cdot \cos 2\varphi] \quad (2)$$

Vector of force  $W$  rotates with variable angular velocity in the direction opposite to the velocity  $\omega$  of driving shaft. Fig. 1 introduces the run of resultant force of inertia  $W$

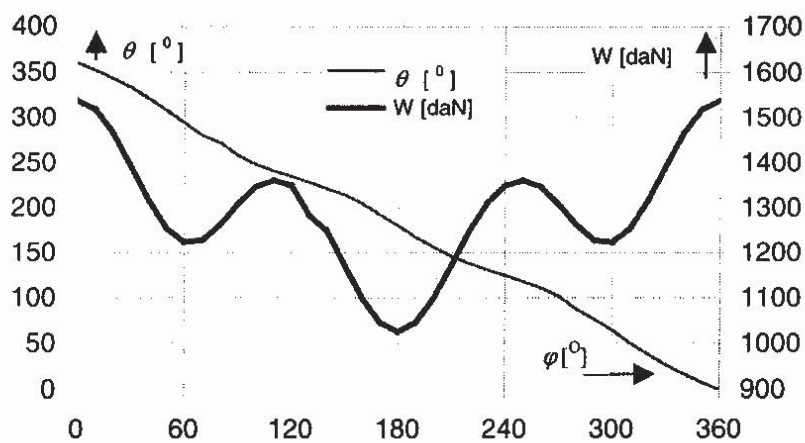


Fig. 1. The run of dynamic loads of needle punching machine main bearing (1st case of load)

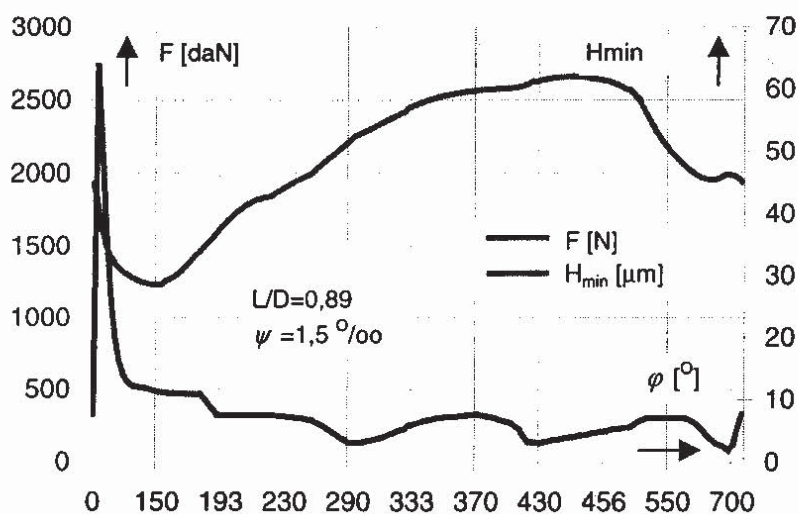


Fig. 2. The run of dynamic loads of engine main bearing and minimum oil film thickness  $H_{min}$

### 3. Journal centre trajectory

The knowledge of journal centre trajectory allows determination of minimum oil film thickness, maximum value of pressure and temperature distributions, i.e. the magnitudes deciding about correct design of journal bearing [1-6]. Bearing clearance, radius of operating surfaces of bush and they displacement with regard to the circle inscribed in the bearing profile as well as the length of bearing are the magnitudes which can be establish on the base of journal centre trajectory.

As result of numerical analysis of dynamically loaded cylindrical journal bearing the oil film pressure distribution, oil film resultant force and journal centre trajectory has been received. The character and value of these loads determines equation (1) and Fig. 1. The classic cylindrical journal bearing with the geometry of lubrication gap given by equation (3) has been assumed for consideration:

$$H(\varphi, z) = H_c + \bar{H}(\varphi) \quad (3)$$

The first part of equation (3) determines the oil film thickness for the cylindrical bearing and has the following meaning:

$$H_c = 1 - \varepsilon \cdot \cos(\varphi - \alpha) \quad (4)$$

where:  $\varepsilon$ - relative eccentricity,  $\varphi$  - peripheral co-ordinate,  $\alpha$  - attitude angle.

Equation (5) determines the oil film thickness in concentric position of the journal and bearing bush axis [2,3].

$$\bar{H}(\varphi) = \psi_s + (\psi_s - 1) \cdot \cos(\varphi - \gamma) \quad (5)$$

where:  $\gamma$  - angle of lobe centre,  $\psi_s$ -the lobe relative clearance,

The journal centre trajectory in the considered journal bearing was determined by numerical solution of Reynolds, energy, viscosity and geometry of oil film equations. The method applied for the solution of: Reynolds, energy, viscosity equations and for determining the journal centre trajectory [1,5] is characterised by the assumptions necessary for describing the phenomena of lubrication and the dynamic of tribological system: journal-lubricant-bearing bush, i.e. adding of pressures at the calculation of the components of hydrodynamic resultant force, and the assumption of non deformable journal and bush.

The method assumes too:

- conditions of heat exchange - isothermal or adiabatic model with the temperature determined from heat balance,
- boundary conditions of oil film - the zones of negative pressures are neglected.

Reynolds equations applied in calculation of journal centre trajectory has the form:

$$\frac{\partial}{\partial \varphi} \left( \frac{H^3}{\bar{\eta}} \frac{\partial \bar{p}}{\partial \varphi} \right) + \frac{\partial}{\partial \bar{z}} \left( \frac{H^3}{\bar{\eta}} \frac{\partial \bar{p}}{\partial \bar{z}} \right) = 6 \left( \frac{\partial \bar{H}}{\partial \varphi} - 2\dot{\varepsilon} \cos(\varphi - \alpha) + \varepsilon \cdot (1 - 2\dot{\alpha}) \sin(\varphi - \alpha) \right) \quad (6)$$

where: D - bearing diameter, L - bearing length, H - dimensionless oil film thickness,  $\bar{H}$  - dimensionless oil film thickness,  $\bar{p}$  - dimensionless oil film pressure,  $\bar{z}$  - dimensionless axial co-ordinate,  $\bar{\eta}$  - dimensionless viscosity of lubricant,  $\dot{\varepsilon}, \dot{\alpha}$  - derivatives of eccentricity and attitude angle with regard to dimensionless time  $\phi = \omega t$ .

The pressure fields computed from equation (6) allows receiving the resultant force  $\bar{F}$  of bearing. Equating the oil film force  $\bar{F}$  to the applied load  $\bar{W}$  yields at any instant [1,5],

$$\bar{W} = \bar{F}\left(\frac{L}{D}, \varepsilon, \alpha, \dot{\varepsilon}, \dot{\alpha}\right) \quad (5)$$

Developed program of calculation with the energy and viscosity equations has allowed the calculation of eccentricity, attitude angle, i.e. the journal centre trajectory in the function of rotation angle of driving shaft. The Runge-Kutta method has been applied for journal centre trajectory calculation [1,5].

#### 4. Results of calculation

The calculation journal centre trajectory have been carried out for the cylindrical and 2-lobe cylindrical journal bearings of diameter  $D = 85$  mm; length  $L = 69$  mm (length to diameter ratio  $L/D = 0,812$ ; journal speed  $n = 1500$  rpm; relative clearance  $\psi = 1,5 \%$  and  $\psi_s = 1,8 \%$  [1,2]. In case of 2-lobe journal bearing, the assumed lobe relative clearance was  $\psi_s = 0,0$ . The case of  $\psi_s = 0,0$  means, that there is cylindrical 2-lobe bearing. The depth of recess was  $10 \mu\text{m}$  and  $20 \mu\text{m}$  and the angle of position  $180^\circ$ , and  $270^\circ$  (Fig.3). Types of considered journal bearings are given in Fig. 3; the 2-lobe bearing shown in Fig. 3b is characterised by symmetric lobe arrangement.

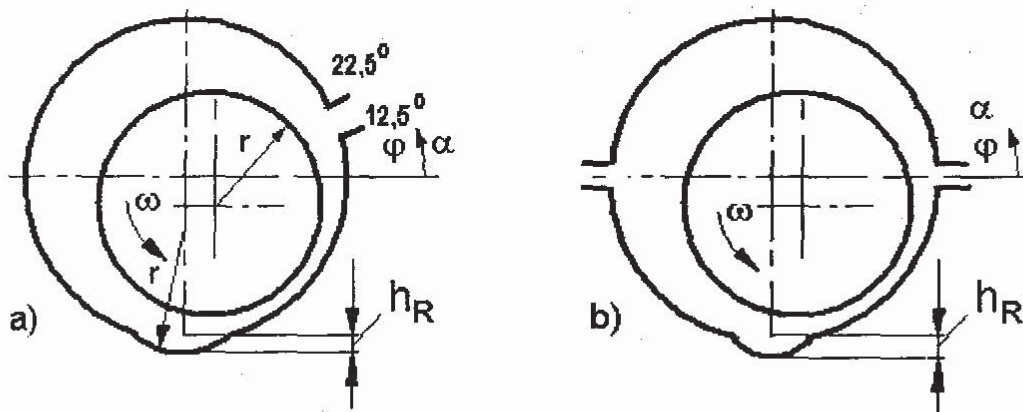


Fig. 3 Bearings considered in the paper: a – cylindrical, b – 2 –pockets;  $h_R$  – depth of recess

Maximum value of load in Ist case of load (Fig. 1) is  $W=15,4 \times 10^3$  N and in the IIIrd case of load the maximum value is  $47 \times 10^3$  N [4,5].

For the load (Ist case) shown in Fig. 1 the results of journal trajectory calculation are shown in Fig. 4 and Fig. 5. On the assumption of similar run of load but with the maximum value of order  $47 \times 10^3$  N, the results are given in Fig. 6 through Fig. 13 for different bearing parameters. For the Ist case of load (Fig. 1) and at different depth of recess the journal trajectories are given in Fig. 4 (at the depth of recess equal  $10 \mu\text{m}$  the maximum value of eccentricity is  $\varepsilon = 0,59794$ ) and Fig. 5 (depth of recess equal  $20 \mu\text{m}$  - maximum value of eccentricity is  $\varepsilon = 0,59567$ ). The analysis of the runs on Fig. 4 and Fig. 5 shows, that the recess has an effect on the journal centre trajectory.

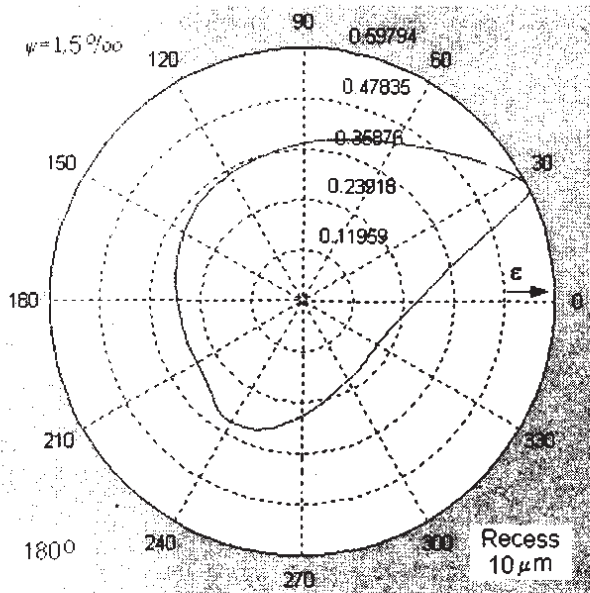


Fig. 4. Journal centre trajectory of cylindrical journal bearing, 1st case of load

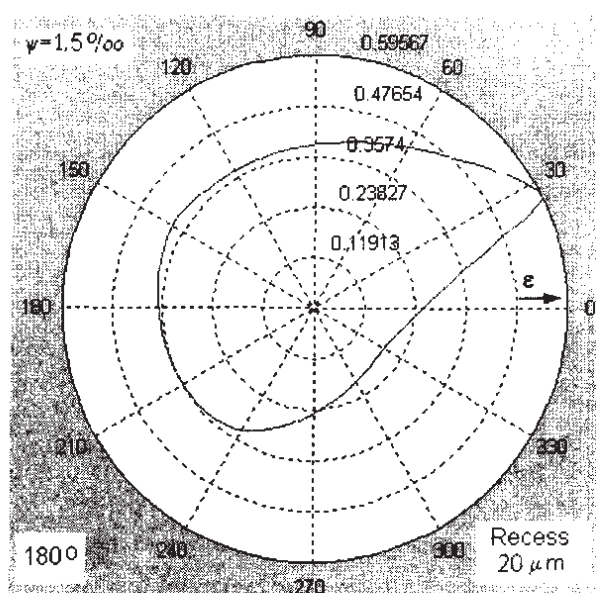


Fig. 5. Journal centre trajectory cylindrical journal bearing 1st case of load

On the assumption of load case No. III, bearing relative clearance  $\psi = 1,5 \text{ ‰}$  and different depth of recess positioned at the angle  $270^\circ$ , the journal centre trajectories can be observed in Fig.6 and Fig. 7. An increase in the depth of recess causes the increase in the maximum value of eccentricity on the trajectory, e.g. at the recess depth equal  $10 \mu\text{m}$  there is and increase in eccentricity from  $\epsilon = 0,79213$  (Fig.6) to the value of  $\epsilon = 0,79466$  at recess depth of  $20\mu\text{m}$  (Fig.7). The run has very similar profile for both assumed depth of recess and the maximum value of eccentricity is placed at the peripheral coordinate equal  $180^\circ$ .

The journal centre trajectories which were obtained at the relative clearance of bearing  $\psi = 1,8 \text{ ‰}$  and at the recess position angle  $180^\circ$  and  $270^\circ$  are introduced in Fig. 8 through Fig. 11. The value of maximum eccentricity  $\epsilon$  of journal centre trajectory is smaller than in case of bearing relative clearance  $\psi = 1,5 \text{ ‰}$  (Fig. 6 and Fig. 10). At assumed depth of recess there is the decrease in the maximum eccentricity on the journal centre trajectory at the increase in the angle of recess position (in Fig. 8 the maximum value is  $\epsilon = 0,67565$  while in Fig. 10 the maximum value of eccentricity is  $\epsilon = 0,66268$ ). The same is in case of larger depth of recess (Fig. 9 and Fig. 11). The run of all trajectories at the relative clearance  $\psi = 1,8 \text{ ‰}$  has similar profile for all considered values of recess depth and the recess position on the bearing peripheral.

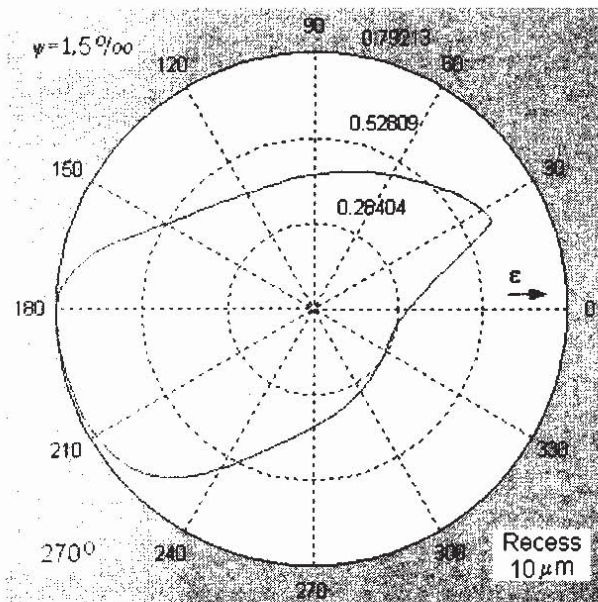


Fig. 6. Journal centre trajectory of cylindrical journal bearing

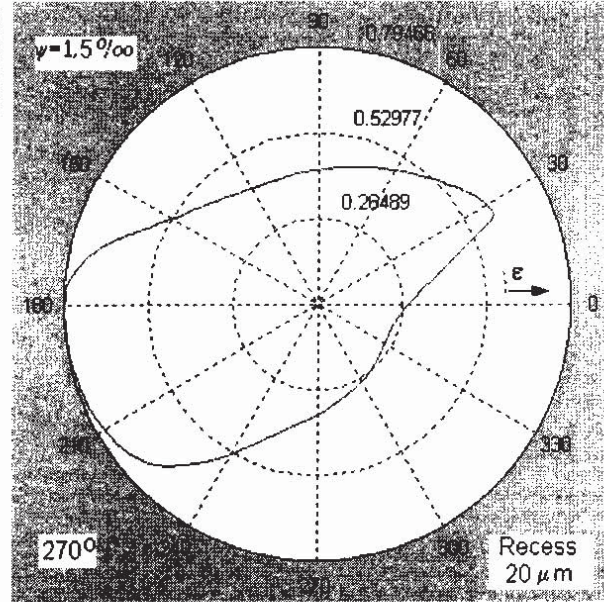


Fig. 7. Journal centre trajectory cylindrical journal bearing

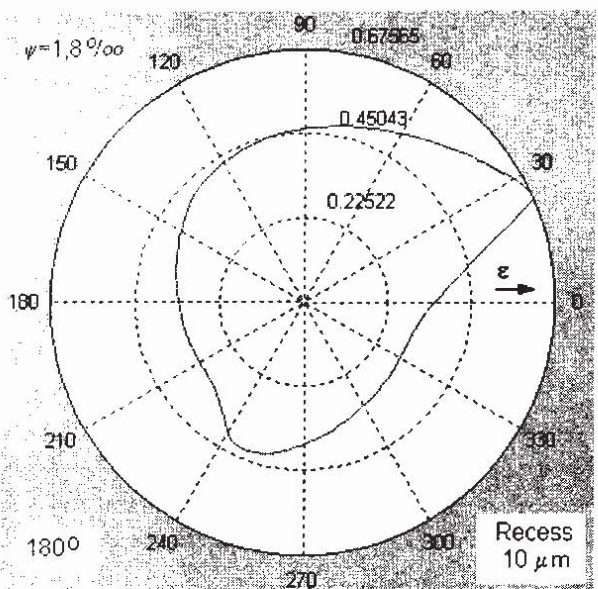


Fig. 8. Journal centre trajectory of cylindrical journal bearing.

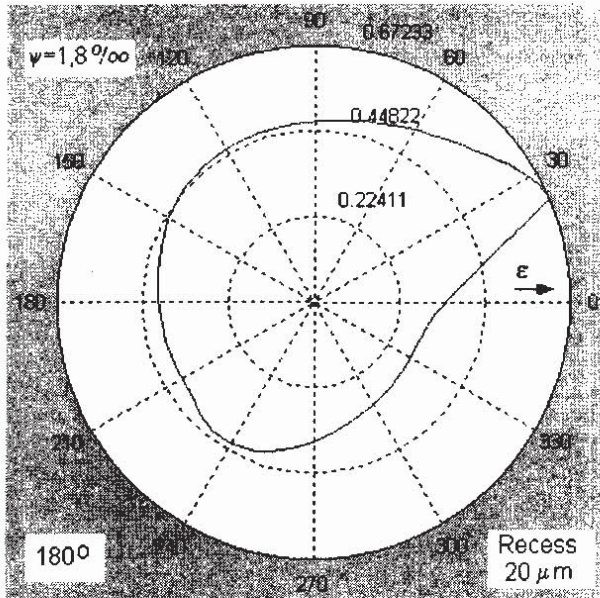


Fig. 9. Journal centre trajectory cylindrical journal bearing

Fig. 12 and Fig. 13 show the journal centre trajectories obtained for the cylindrical journal bearing at the dynamic load corresponding to the load of main bearing of internal combustion engine (Fig.2). Relative bearing clearance  $\psi = 1,5 \text{ ‰}$  has been used and the angle of recess position was  $270^\circ$ . The recess changes the shape of journal centre trajectory; at the depth of recess equal  $10 \mu\text{m}$  the maximum value of trajectory eccentricity is  $\epsilon = 0.53185$  (placed at the peripheral coordinate  $\varphi = 230^\circ$  – Fig. 12). An increase in the depth of recess to  $20 \mu\text{m}$  causes the increase in maximum value of eccentricity to  $\epsilon = 0,54959$  and moves the position of this value to the peripheral coordinate  $\varphi = 220^\circ$  ( Fig. 13).

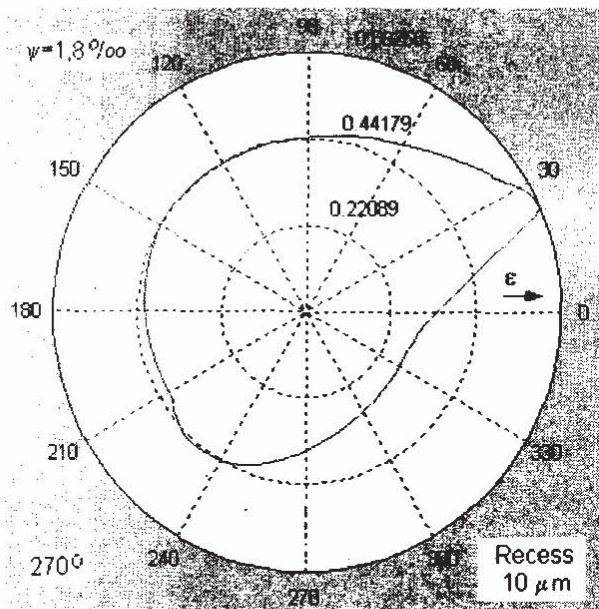


Fig. 10. Journal centre trajectory of cylindrical journal bearing,

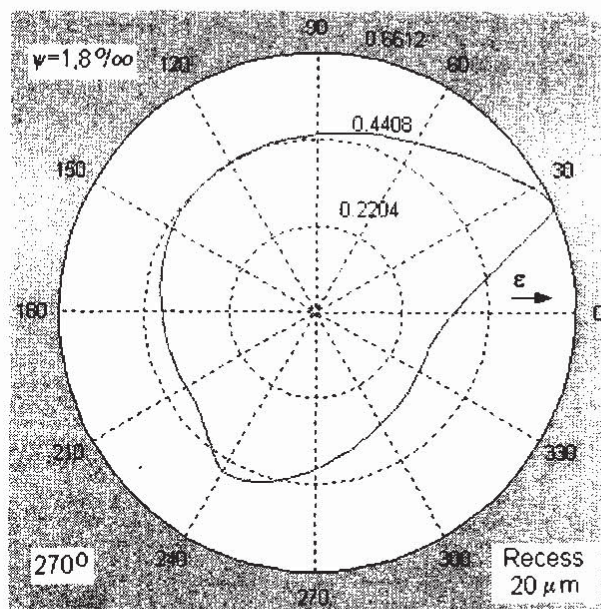


Fig. 11. Journal centre trajectory cylindrical journal bearing

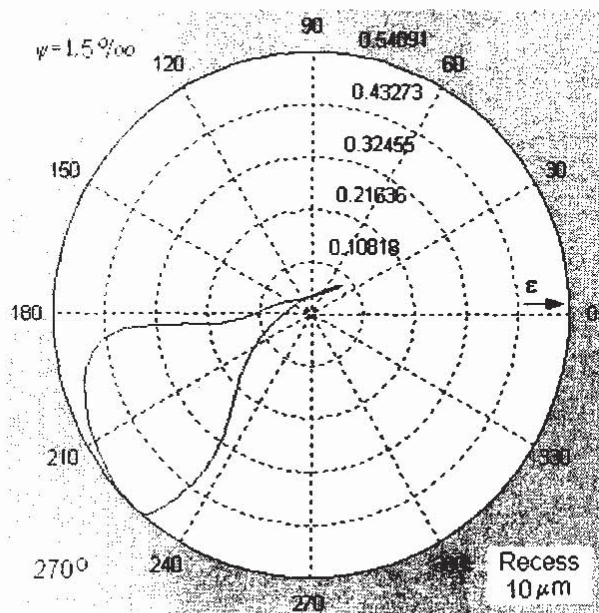


Fig. 12. Journal centre trajectory of cylindrical journal bearing, (dynamic load - Fig. 2)

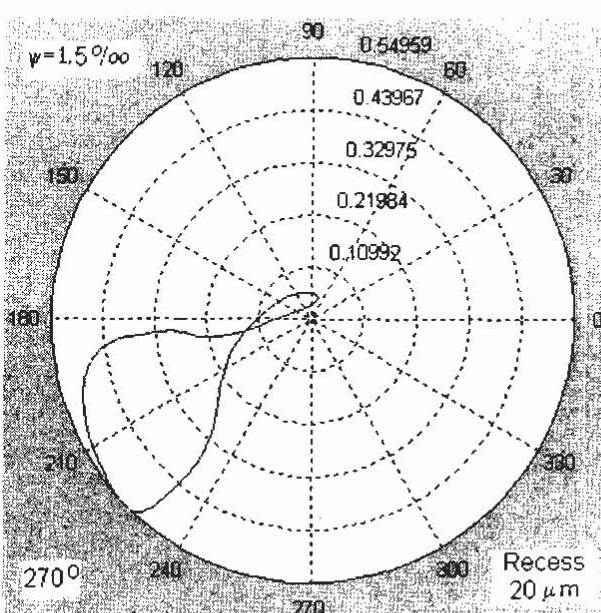


Fig. 13. Journal centre trajectory cylindrical journal bearing ( dynamic load - Fig.2)

In case of 2-lobe journal bearing with cylindrical profile of lobes, the shapes of journal centre trajectories, obtained at the IIIrd case of load (Fig. 1), are shown in Fig. 14 and Fig. 15. The journal centre trajectories are larger than in case of cylindrical journal bearing and they have the shape of deformed ellipse. This deformed shape is caused by the presence of two oil grooves arranged at the peripheral coordinates  $\varphi = 0^\circ$  and  $\varphi = 180^\circ$ . At assumed bearing relative clearance  $\psi$  and the angle of recess position equal  $270^\circ$ , an increase in the depth of recess causes the decrease in the maximum value of eccentricity (Fig. 14 -  $\epsilon = 0.72494$  at the depth of recess equal  $10 \mu\text{m}$  and Fig. 15-  $\epsilon = 0,72007$  at the depth of recess equal  $20 \mu\text{m}$  ). There is also an increase of the smaller axis of deformed ellipse, which can be observed on the line between peripheral coordinates  $\varphi = 120^\circ$  and  $\varphi = 300^\circ$  -e.g. Fig. 14.

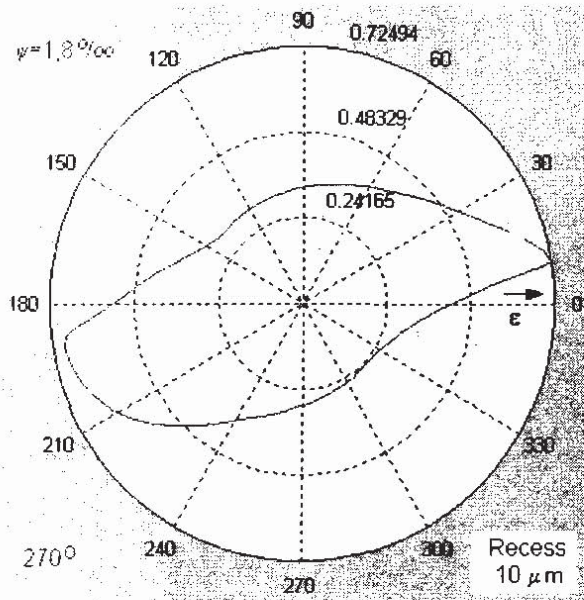


Fig. 14. Journal centre trajectory of cylindrical 2-pockets journal bearing.

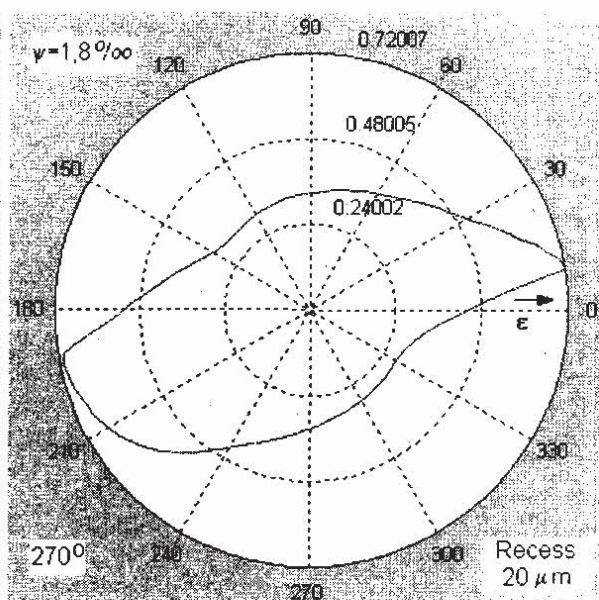


Fig. 15. Journal centre trajectory cylindrical 2-pockets journal bearing

## 5. Conclusions

As result of the calculation of journal centre trajectories for different dynamic loads and depth of recess, below given conclusions can be introduced.

1. The profile of journal centre trajectory for considered journal bearings is affected by the recess in bearing bush.
2. The angular position of recess on the bearing peripheral and the bearing relative clearance affects the journal centre trajectory.
3. Applied method of calculation and developed program allows the calculation and analysis of cylindrical and multilobe journal bearings with the recess.

## References

- [1] Kapusta H., Strzelecki S.: *Numerical Analysis of Needle Punching Machine Journal Bearings Operation*. VI International Textile Conference IMTEX'2000. Lodz 2000. Włókiennictwo. Scientific Bulletin of Lodz Technical University. No. 58.2000. 341-347.
- [2] Schaffrath, G., *Das Gleitlager mit beliebiger Schmierspaltform- Verlagerung des Wellenzapfens mit zeitlich veränderlicher Belastung*. Diss. T.U. Karlsruhe. 1967.
- [3] Someya, T., *Das dynamisch belastete Radial-Gleitlager beliebigen Querschnitts*. Ingenieur Archiv, Bd.34, Nr.1. 1953.
- [4] Strzelecki S., Kapusta H., *Application of Multilobe Journal Bearings in the Needle Punching Machine*. Synopses of 2nd World Tribology Congress, 6-7th September 2001. Vienna, Austria. 2001. 406.
- [5] Strzelecki S., Someya T., *Maximum Oil Film Pressure and Temperature of Dynamically Loaded Journal Bearing*. Proceedings of the 5th International Tribology Conference. 6-9 December 1998. Brisbane, Australia. 1998. 219-224.